Researchers Journal of Science and Technology (REJOST)
https://rejost.com.ng

Application of Seismic and Well Log Data Integration Workflow for Reservoir Characterization of the "ABU" Field, Niger Delta, Nigeria

Abraham C. Udoh[1], Camillus E. Etim[1], Monday U. Udoh[2], Augustine I. Chinwuko[3], Aniekan E. Ekpo[1], Ayatu O. Usman[4] and Olatunbosun Olagundoye[5]

Abstract

This study applies a data integration workflow to structurally, stratigraphically, and petrophysically characterize the "ABU" Field in the Niger Delta. The analysis focuses on fault mapping, reservoir delineation, and hydrocarbon potential assessment. Using variance attribute techniques, 15 faults were identified—12 synthetic and 3 antithetic—with a major antithetic fault forming a graben structure in the ABU-2 area. These predominantly listric faults are characteristic of Niger Delta growth fault systems and act as key structural traps. The major growth fault trends northeast–southwest, consistent with regional tectonics. Sequence stratigraphy reveals two third-order depositional cycles associated with transgressive marine settings, and three dominant facies: channel sands, upper shoreface sands, and shales. Reservoir mapping delineates three main reservoirs (B, C, and G). Reservoir G, characterized by a well-defined anticlinal closure, exhibits the highest hydrocarbon potential. Petrophysical analysis shows that Reservoir G has a Net-to-Gross ratio ranging from 0.25 to 0.93, porosity between 29% and 33%, and permeability from 153.79 mD to 579.11 mD. Reservoir B demonstrates slightly higher porosity (30% to 33%) and permeability (200.58 mD to 472.83 mD), but higher water saturation reduces its hydrocarbon potential. Reservoir C has lower reservoir quality, with Net-to-Gross values between 0.25 and 0.77, porosity from 28% to 32%, and permeability between 160.45 mD and 432.10 mD, accompanied by higher water saturation. Overall, the ABU Field shows considerable hydrocarbon potential, particularly in Reservoir G. Variations in reservoir quality are largely influenced by growth fault architecture and depositional environments.

✉ Abraham C. Udoh: abrahamudoh@aksu.edu.ng

[1] Department of Geology, Akwa Ibom State University, Mkpat Enin L.G.A., Nigeria.

[2] Pioneer-Alfa Petroleum Services Ltd, Benin City, Edo State, Nigeria

[3] Department of Applied Geophysics, Nnamdi Azikiwe University, Awka, Nigeria.

[4] Department of Geology/Geophysics, Alex Ekwueme Federal University, Ndufu-Alike, Ebonyi State, Nigeria.

[5] TotalEnergies EP Nigeria Limited, Lagos, Nigeria.

Keywords: Reservoir Characterization; Fault Mapping; Hydrocarbon Potential; Sequence Stratigraphy; Petrophysical Analysis.

Article history
Received: March 21, 2025
Received in revised form: June 6, 2025
Accepted for publication: June 11, 2025
Available online: June 12, 2025

1.0 Introduction

Deltas are "discrete shoreline protuberances formed where rivers enter oceans, semi-enclosed seas, lakes or lagoons, and supply sediment more rapidly than it can be redistributed by basinal processes" (Boggs, 2006). Deltas are therefore most significant in the open ocean, although they can also form in lakes and interior seas. Deltas are where a large portion of the siliciclastic silt that has been carried to coastal zones over geologic time has been deposited. Typically, well-defined drainage networks that feed sediment to a limited portion of the shoreline and terminate in a trunk stream serve deltas, causing a depocenter to form. (Reading, 1986). Since deltas are frequently important depocentres (Figure 1) throughout the geological column, they create remarkable dense sequences that have been identified. Waves, tides, and ocean currents are examples of basin processes that can help spread sediment and rework silt that has been deposited by river currents. Numerous features of deltas are the outcome of this interaction between basinal and fluvial processes. Major deltas have a variety of tectonic settings, but the most prevalent ones include cratonic basins, foreland basins or marginal basins connected to mountain ranges, and passive continental edges (like the Niger delta). For a variety of reasons, deltas are frequently important hydrocarbon provinces. Sands, which are potential hydrocarbon reservoirs, can be transported far out into muds rich in organic matter in marine basins, which are possible beds of hydrocarbon sources, via the deltaic process (Selley, 1980). Because deformation of the structure creates traps for migratory hydrocarbons, deltas frequently occur in regions of crustal instability. Additionally, deltas create their own traps in rollover anticlines, growth faults, and related traps. Either laterally sealed structures created by the juxtaposition of shale units against reservoir sands over growth faults or vertically sealed rollover anticlinal structures are the most common structurally based hydrocarbon-trapping mechanisms in the delta. (Doust and Omatsola,1990).

In general, faults are crucial to the distribution of hydrocarbons. Growth faults (Figure 2) might possibly serve as routes for the movement of hydrocarbons from the overstressed marine clays. The delta's structural structure is dominated by growth faulting, which becomes more complex as one moves seaward. (Udoh *et al*., 2020). Stratigraphic traps are not unusual, though. Stratigraphic traps are just as likely to occur on the delta's flanks as structural traps (Beka and Oti,1995). These traps are created when impermeable shales terminate the sand facies laterally or vertically. The Niger Delta's subsurface reservoir facies vary quickly over shallow depths and short distances due to wave dominance and the series of multiple transgressive and regressive cycles and episodes. This makes it difficult to locate reservoirs, define their internal structure and shape, and ultimately create the best energy for the purpose of exploitation. (Aminu and Olorunniwo, 2011). Oil and gas may exist in a region in appreciable quantities and yet be inaccessible in practical and commercial terms. Albeit, there are a number of causes of this circumstance, one of the most common and discouraging is the lack of any rock formation, in suitable stratigraphic position, possessing both the porosity and the permeability necessary both to contain and to yield oil, or gas, or both, in commercial quantities. Any rock capable of

performing these functions is a reservoir rock (North, 1990). Sandstone reservoir characteristics are determined by the primary composition, which is governed by the diagenetic processes that occur close to the surface and during burial, as well as the depositional environment's textural and mineralogical composition (provenance) (Bjorlykke, 2015). In essence, "reservoir characterization" refers to all the relevant data needed to characterize a reservoir with regard to its capacity to generate and store hydrocarbons. (Chopra and Michelena, 2011). This means being aware of the reservoir's entire architecture, encompassing its external and interior geometry, its dynamic fluid flow, and its model with the distribution of its static attributes (such as porosity, permeability, heterogeneity, and net pay thickness, among others). Such data reduces expensive investment, revitalizes oil fields, predicts the performance of future reservoirs, increases production rates, and aids oil company management in creating precise financial models. The technical domains of data management, petrophysics, reservoir engineering, geology, geophysics, and economics are all integrated in reservoir characterization, which is regarded as a crucial stage between an oil or gas field's discovery and the reservoir management stage.

In order to characterize the reservoir and predict the depositional environment within the "ABU" Field, which is located offshore in the eastern Niger Delta of Nigeria (Figure 1), this study intends to combine 3D seismic data with well logs. The objectives were to assess the structural components influencing hydrocarbon distribution in the ABU field and to elucidate the reasons for the deficiency of hydrocarbons at anticipated levels. Knowing the depositional and facies environment and the geological data that are currently accessible are typically the first steps in any reservoir characterization process. A sequence stratigraphic method and structural interpretation of seismic data are crucial inputs that define the reservoir model's framework. Numerous generated seismic features and their alignment with relevant rock physics models and log data provide the seismic data's contribution to the petrophysical parameters of 3D reservoir models. (Chopra and Michelena, 2011).

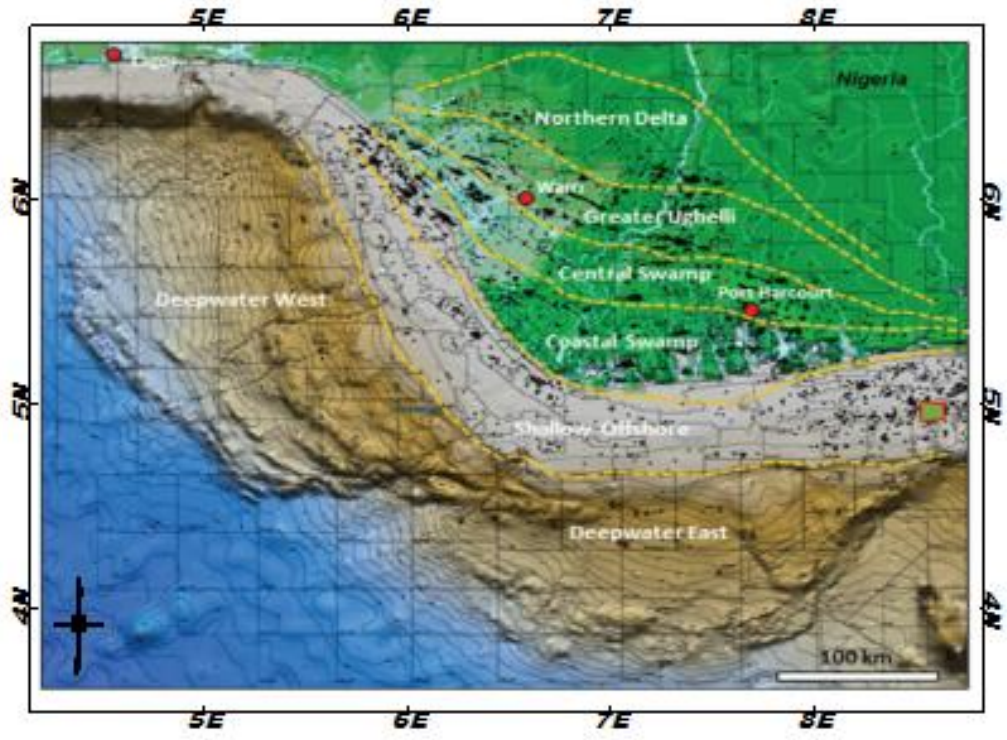


Figure 1: The Niger Delta's bottom topography and shaded relief, along with an approximate delineation of the main depobelts (Adapted from Wojcik *et al.*, 2016). The Study Area is inscribed as a red rectangle

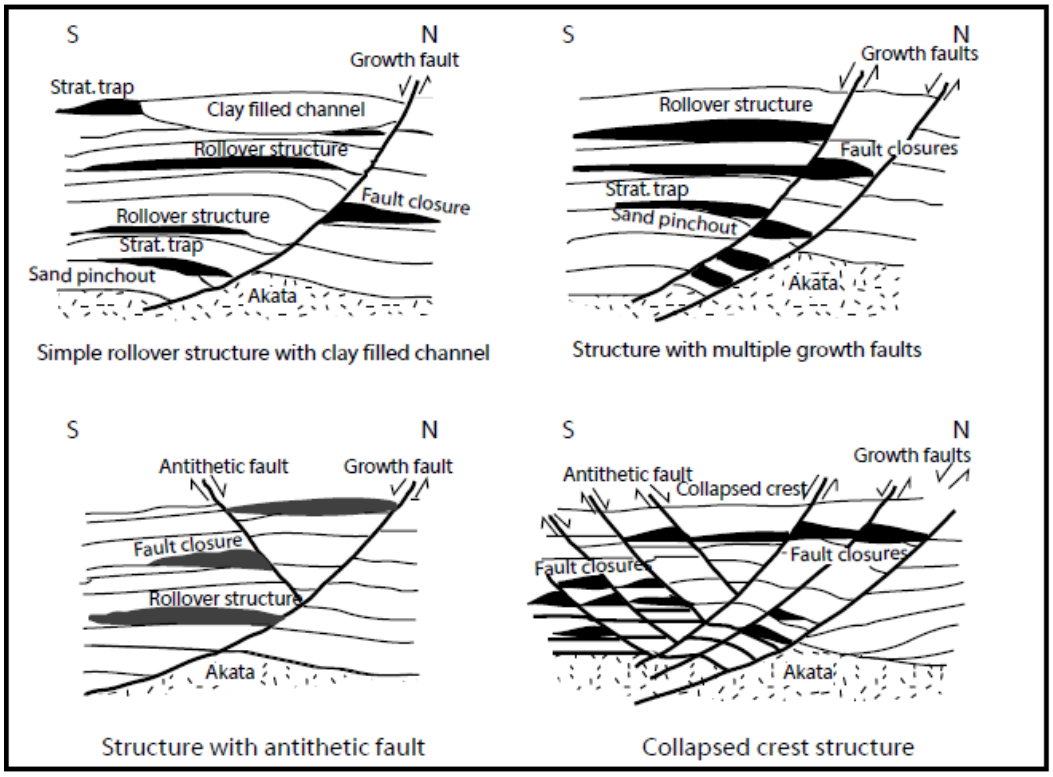


Figure 2: The Niger Delta's oil field architecture and associated trap types (Doust and Omatsola, 1990; Stacher, 1995).

2.0 Geological Setting

The end of the Benue Trough is where the Niger Delta Basin is located in the eastern portion of the Gulf of Guinea. The rifting and opening of the South Atlantic during the Late Jurassic to Mid-Cretaceous, followed by its shift to a passive border setting in the Late Cretaceous, is associated with the Trough, a failed arm of a triple junction (Burke et al., 1971). Progradation and extension of a sizable sedimentary wedge of the Niger Delta caused by gravity, with a maximum thickness of more than 12 km, dominates the Tertiary development of the margin. (Doust and Omatsola, 1990). The Rivers of Niger and Benue, which drain a sizable portion of the African Craton, dominate the Niger Delta's sediment delivery system. This mechanism was established early on in the margin's history and has been providing the Delta with sediments rich in quartz from the African Craton since the Late Cretaceous. (Doust and Omatsola, 1990). The lithostratigraphic succession of the Niger Delta is divided into three major units(Short & Stauble,1967) comprising the Akata Formation's marine shales at the system's base, the Agbada Formation's paralic arrangement of shales and sandstones, and the sand-rich, riverine series of the Benin Formation (Doust & Omatsola, 1990).The Agbada Formation, the promising interval, has several sandstone/shale cycles that produce efficient reservoir/seal pairings and allow hydrocarbons to be trapped. (Figure 3).

Through the intercalations of sand, shale, silt, and/or sandstone sides, these formations demonstrated analogs of the delta plain, delta front, and prodelta habitats (Udoh *et al*., 2017). The Agbada Formation contains the majority of the Niger Delta's hydrocarbon potential (Doust and Omatsola, 1990) typically trapped within rollover anticlines that are linked to growth faults(i.e., simple rollover and hanging-wall closures have the most gas volumes, whereas faulted anticlines, where the fault may have been gas leakage pathways, have the biggest oil amounts, leaving oil in the traps) (Udoh and Udoh, 2020).The outboard deep-water region has conventional slope and toe-of-slope turbidites, whereas the shallow offshore region and the onshore depobelts are mainly shallow

marine and deltaic systems (Figure1). The development of the Niger Delta was controlled by large-scale synsedimentary growth faults and counter- regional faults, which separated the system into several fault-bounded depobelts (Doust and Omatsola, 1990). The delta top deposit moves ahead of the Agbada deposits during a significant progradational event.

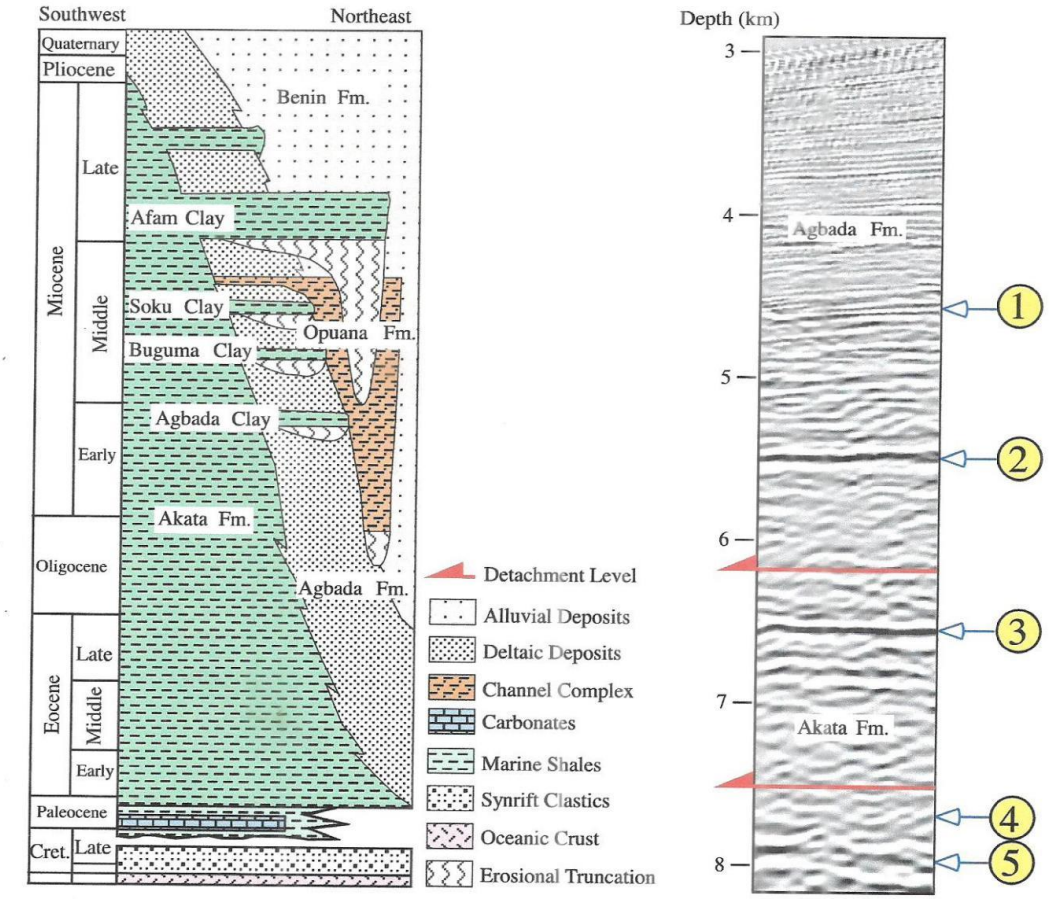


Figure 3: Regional stratigraphy of the Niger Delta is represented diagrammatically, and the main stratigraphic units in the thrust belt, outer fold, and principal reflectors are shown using variable density seismic display. They include: (1) the Agbada Formation's summit, (2) the Akata Formation's summit, (3) mid-reflection on Akata, (4) thought to be on top of the clastic deposits of the synrift, and (5) top of the oceanic crust. Red arrows indicate the main detachment levels. The stratigraphic segment has been altered from Lawrence et al. (2002).

A new, younger depocenter is created when sedimentation of Agbada deposits moves towards this formerly distal realm and new depobelts' bordering faults form under the influence of sediment loading. Meanwhile, the older depobelt is abandoned and covered by Benin Formation fluvial deposits. Therefore, each depobelts placement is determined by major regional faults (Udoh *et al*., 2017).

Sedimentation in deltaic and most depositional environments is made up of stratigraphic cycles that are mainly defined by the switching between materials that are supplied with energy and those that are not, like changes between sand and shale (e.g., Damuth, 1994; Edwards, 1995; Cross and Lessenger, 1998; Soreghan *et al*., 1999). Due to growth faulting, the different processes may respond differently to differential subsidence: The uniform distribution of sedimentation across faults is caused by decantation, or the nondynamic settling of shale particles (Lowrie, 1986; Cartwright et al., 1998) without spreading over tens to hundreds of thousands of years to topographic lows (Mitchell, 1996; Webb and Jordan, 2001); however, dynamic deposition (sands) fills up the lows before deposition takes place on the highs.

3.0 Materials and Methods

3.1 Well logs

Three wells (ABU-1, ABU-2, ABU-3) were drilled in the field with ABU-1 penetrating two shallow reservoirs and ABU-2 penetrating a deeper reservoir (Figure 4). Open hole logging was conducted in all the wells and the logs acquired were of same vintage. In summary, there is a good coverage of gamma, resistivity, Sonic, neutron and density logs except paucity of neutron and density log in ABU-3 (Table 1). No PVT, Side wall core samples and full-bore core samples were given for any of the reservoirs of interest.

Before the logs were used for petrophysical studies, facies identification, etc, log quality control (QC) was done using the standard techniques. In sum, the quality of the data utilised for this study was satisfactory. Basically, neutron and density logs were used for fluid typing and definition of contact as PVT data was not available, thus an uncertainty may be incurred. For seismic to well tie and subsequent time-depth relationship, checkshot data for ABU-1, 2 and 3 were used.

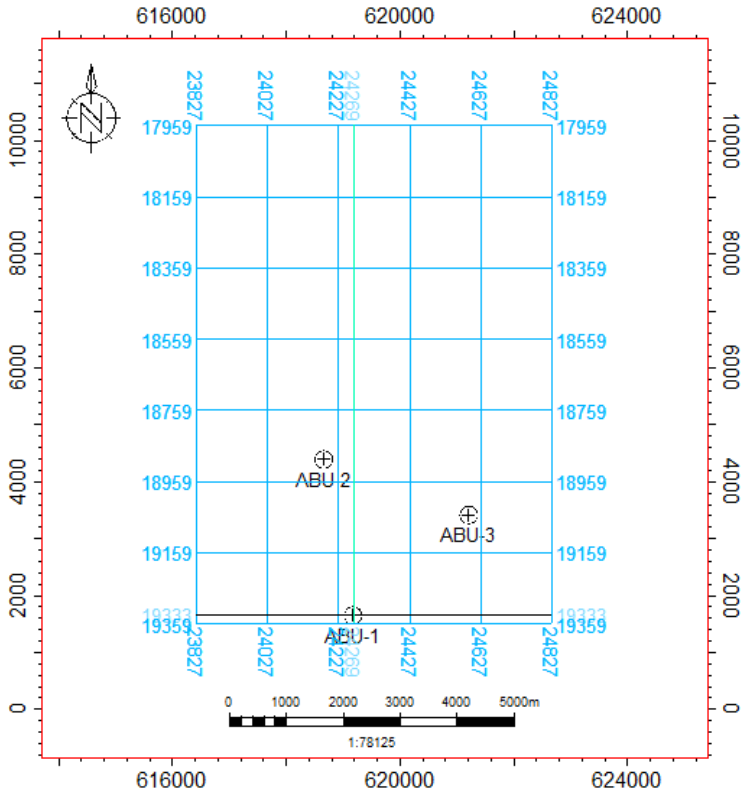


Figure 4: Base concession map showing well trajectory and Seismic coverage

Table 1: Well and well log inventory

Well	Gamma	Caliper	Resistivity	Density	Sonic	Neutron
ABU-1	✓	✓	✓	✓	✓	✓
ABU-2	✓	✓	✓	✓	✓	✓
ABU-3	✓	✓	✓	X	✓	X

✓ - Available, X – Not Available

3.2 3D Seismic data

The 3D seismic data utilized in this study covered about 54.7sqkm in ZGY format. The data mirrors structures and stratigraphy of the field within 9s window seemingly beyond the Akata formation of the Niger Delta. It was sampled at 4ms and processed at a bin grid of 12m x 12m. Walking through the seismic data, a

dominant frequency of 24Hz was observed although the overall frequency ranges from 0 – 250Hz. In sum, the quality of the seismic is reasonable with a signal to noise crossover frequency of 25Hz. The representative reservoir surfaces were mapped across the 3D seismic data following their corresponding seismic reflections.

3.5 Methodology

Figure 5 shows the workflow that guided the analysis.

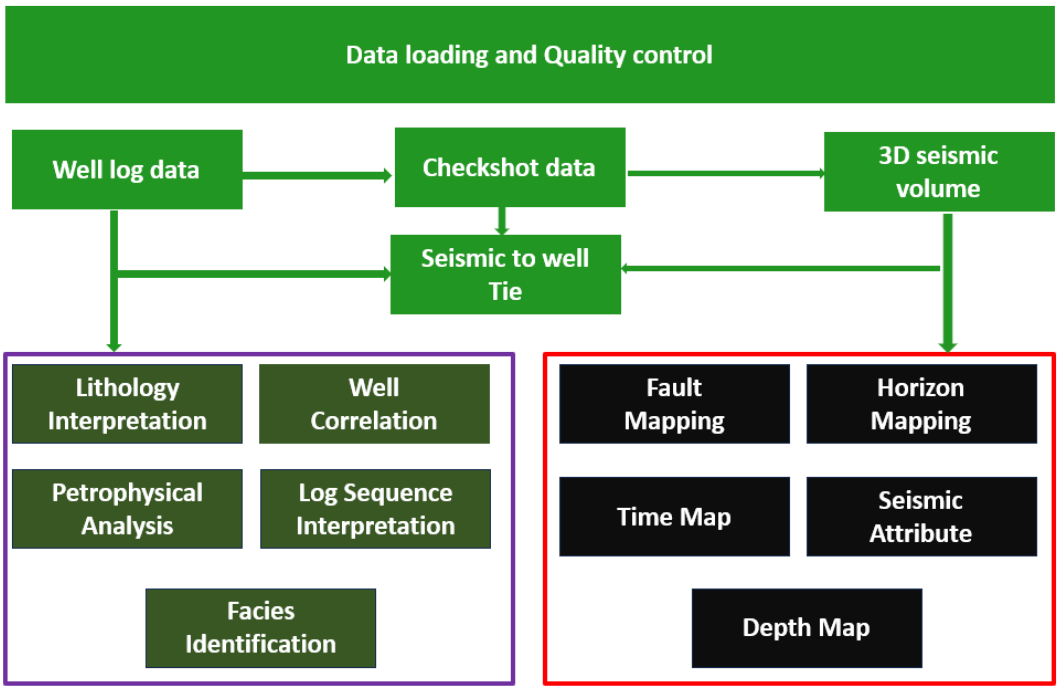


Figure 5: Workflow

3.3 Stratigraphic correlation

Using gamma ray logs with a sand cut-off of 60API across the three wells, lithologies were delineated, and a stratigraphic correlation was carried out across ABU-1, ABU-2 and ABU-3 (Figure 6). Furthermore, reservoirs were identified using resistivity log and fluid typing logs (neutron and density logs) and formation tops were confirmed using Water Saturation and porosity logs (Figure 7).

3.4 Identification of Facies

Due to the lack of core data, the facies were identified using the log motif. Finning upward sequences were interpreted as channel systems, blocky signatures as channels, and coarsening upward sequences (Funnel shape) as shoreface systems based on the interpretation of the gamma ray logs (Cant, 1992). Additionally, the degree of cleanliness of the sand packages determined the classification into lower and upper shoreface, channel, and channel heterolith (Figure7).

3.6 Petrophysical Evaluation

Utilizing the necessary wireline log – Five petrophysical parameters- porosity (ø), Net-to-Gross (NTG), Volume of Shale (VSH), Water Saturation (S_W) and Permeability (mD) were characterized in this study. The density log was used to determine total porosity ($ø_T$) in the examined clastic interval, assuming a matrix density value of 2.65 g/cc. To estimate effective porosity ($ø_e$) from Total porosity ($ø_T$), an adjustment for shale volume was implemented. Water Saturation (S_W) and Permeability were obtained using Archie's equation and Timur equation, respectively.

Despite the fact that log-based petrophysical parameters are usually validated and calibrated using core-based direct measurements, core-based petrophysical data were not available for this study.

3.7 ABU Field Well -To- Seismic Tie

Following quality checks, a thorough seismic to well tie exercise was conducted using 3D

seismic data, Checkshot velocity data, sonic log, and modeled density log from the ABU-1 well (Figure 9). By combining the dominant frequency of the 24 Hz wavelet extraction from the seismic at the well location with the reflectivity coefficient produced by a series of acoustic impedance contrasts constructed by multiplying Checkshot-calibrated sonic and density, a synthetic seismogram was calculated. Following equilibrium in the lobe symmetry of the wavelet between the synthetic and seismic seismograms, a good tie was obtained after iterative parameter testing. Additionally, in accordance with seismic in zero phase, the synthetic seismogram was rotated 180 degrees.

3.8 Time structural Map Generation

With a dense mapping of 10x10ms across Inlines and Xlines, seeded horizons corresponding to the three reservoirs of interest were used as input to generate TWT structural map. Furthermore, the TWT maps were used as inputs for amplitude extraction. The amplitude maps were quality-checked to ascertain their conformity to structure and other geological undertones. However, RMS and Minimum amplitude were employed to mirror reservoir geophysics.

3.9 Time and Depth Generation

Using a less robust velocity model (Polynomial – 2nd Order) the time maps were translated into Depth structural maps for further subsurface evaluations. Following depth conversion, the models were constrained using harmonized well tops (markers) at well penetrations.

4.0 Results

Using the methodology above, the results of the geological, geophysical and petrophysical analysis of the identified reservoirs are presented below. These include, the well log correlation panel (Figure 6), delineation of reservoir formation tops (Figure 7), sequence stratigraphy and facies identification (Figure 8), synthetic seismogram (Figure 9), coherency map (Figure 10), time map, depth map, Root Mean Square (RMS) map and minimum amplitude map (Figures 12 – 23).

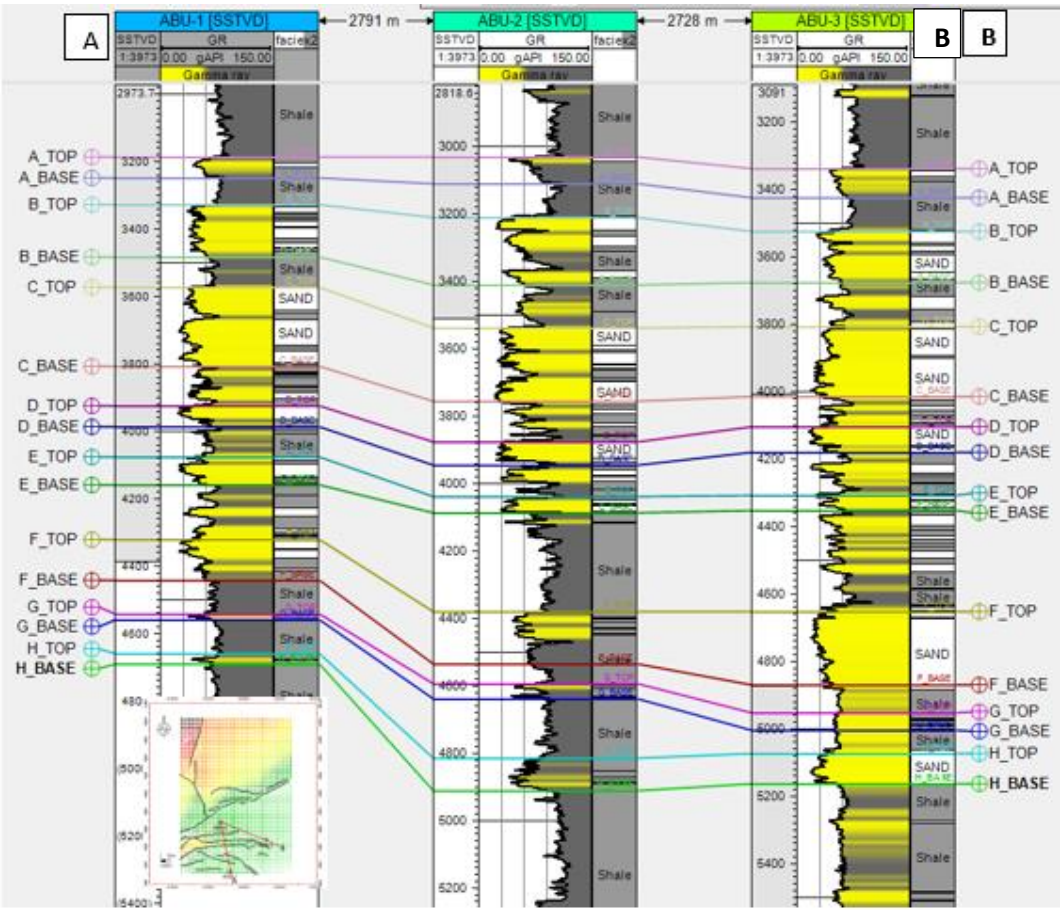
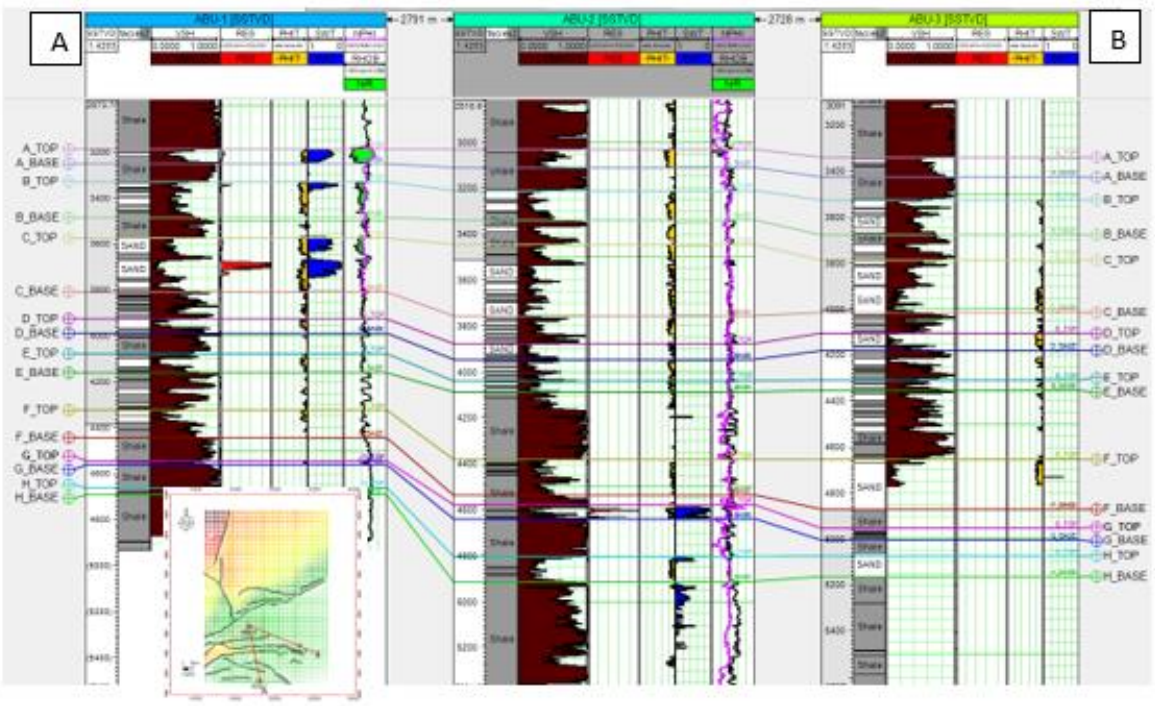


Figure 6: Well log Correlation (sand cut-off: 60API)



Track1: Volume of Shale log; Track 2: Resistivity; Track 3: Total Porosity; Track 4: Water Saturation; Track 6: Neutron Porosity/Bulk Density logs

Figure 7: Formation tops (Showing Reservoirs B, C and G)

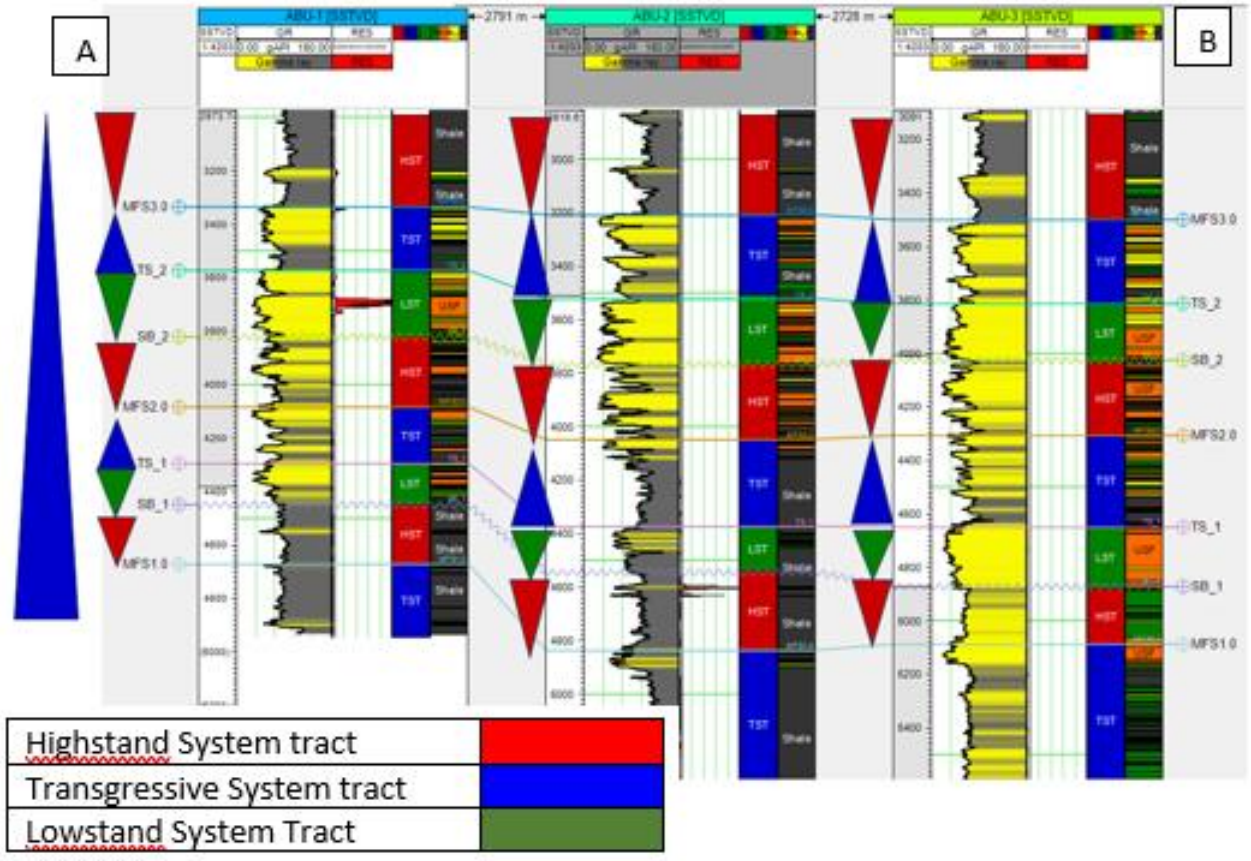
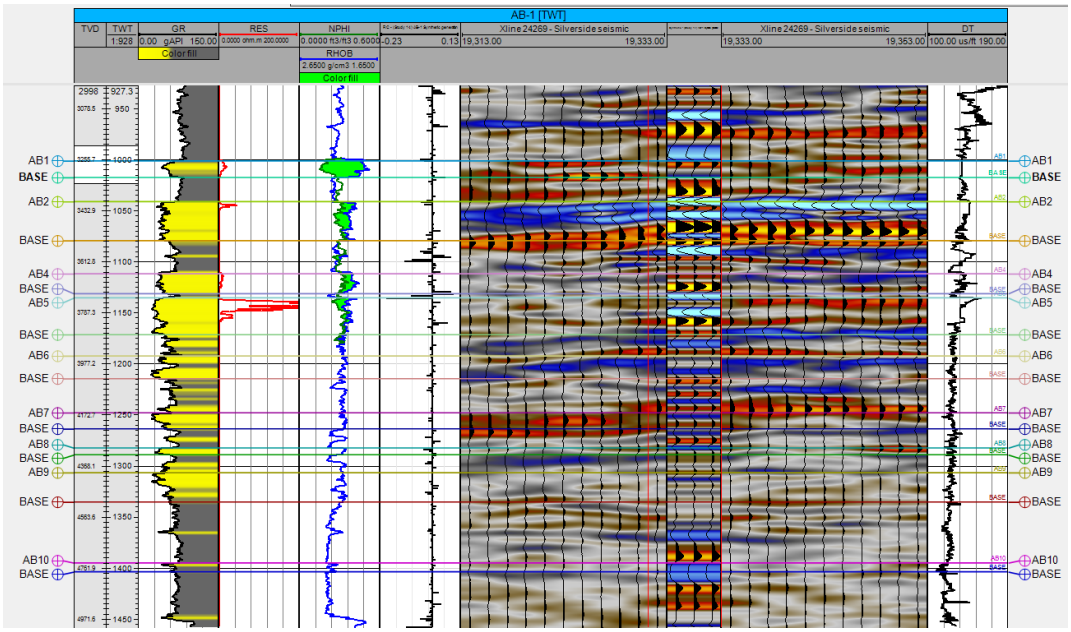
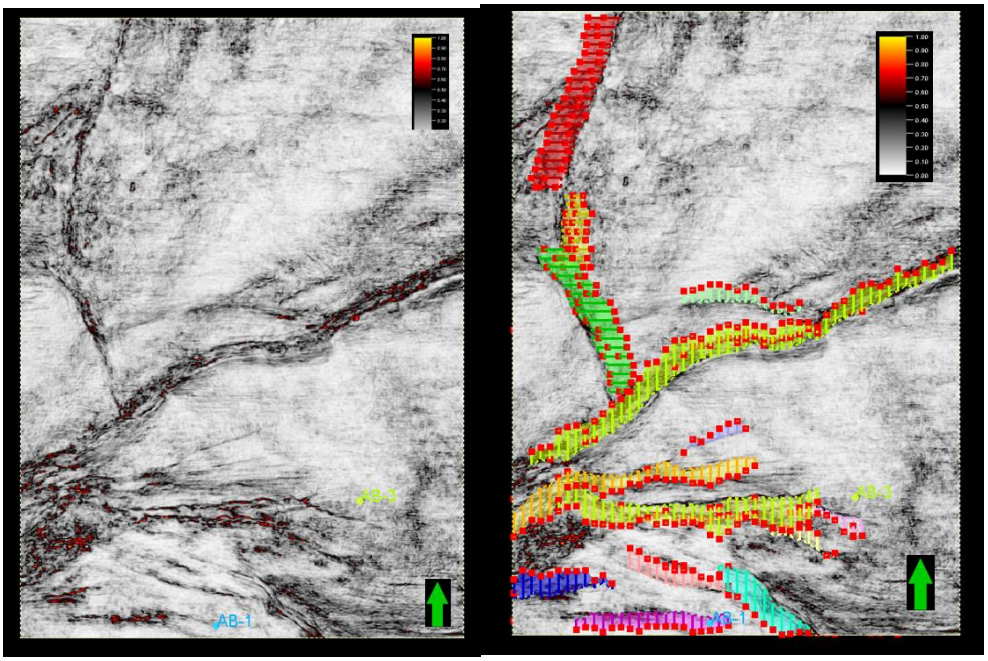


Figure 8: Sequence Stratigraphic framework of ABU field/ Facies Identification



Track 1: Gamma ray log; Track 2: Resistivity Log; Track 3: Neutron log/ Bulk density log; Track4: Reflectivity Coefficient; Track 5: Field seismics/synthetic seismics; Track 6: Sonic log

Figure 9: Synthetic Seismogram along AB-1



(a) (b)

Figure10: Coherency map (@1100ms): (a) uninterpreted (b) Interpreted (Showing fault polygon)

Reservoir B

Reservoir B time, depth, Root Mean Square (RMS) and minimum amplitude are presented below.

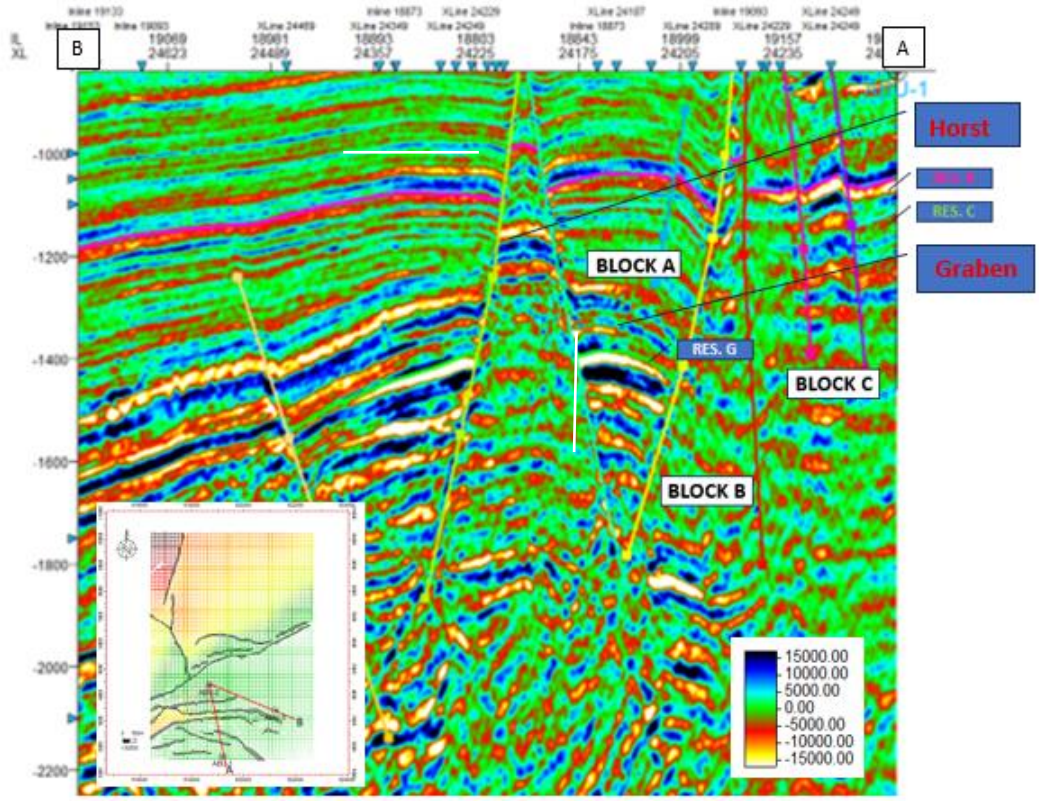


Figure 11: Acoustic impedance seismic section along wells ABU-1, ABU-2 and ABU-3 showing reservoir continuity from ABU-1

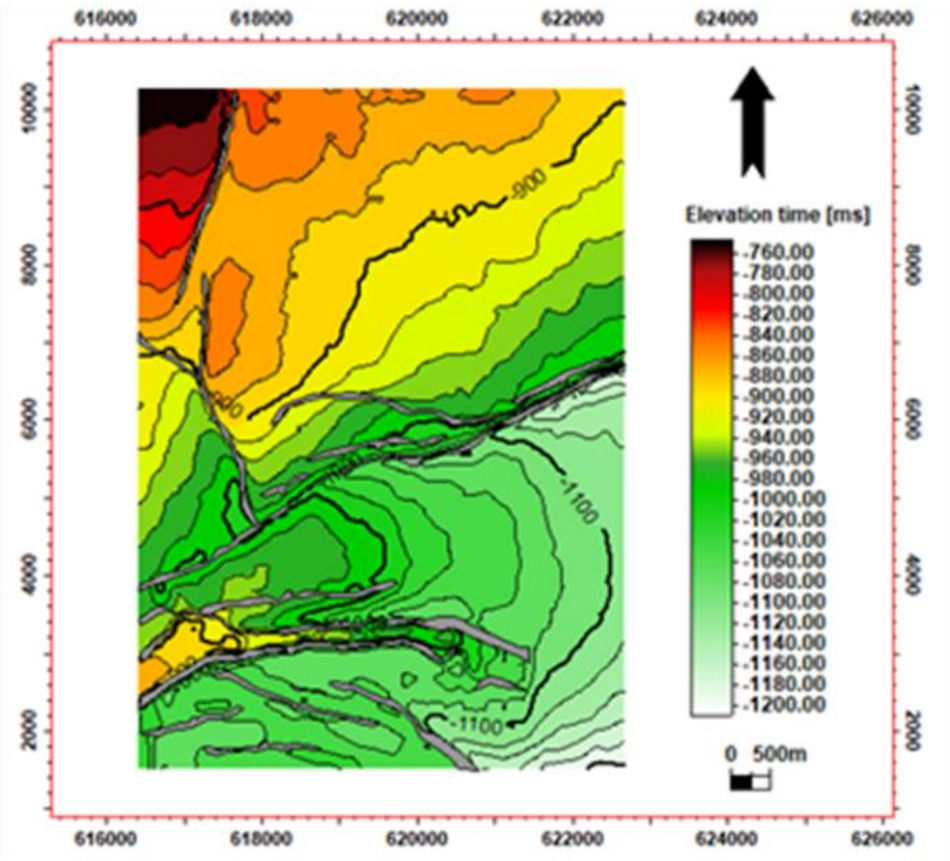


Figure 12: Reservoir B Time Map

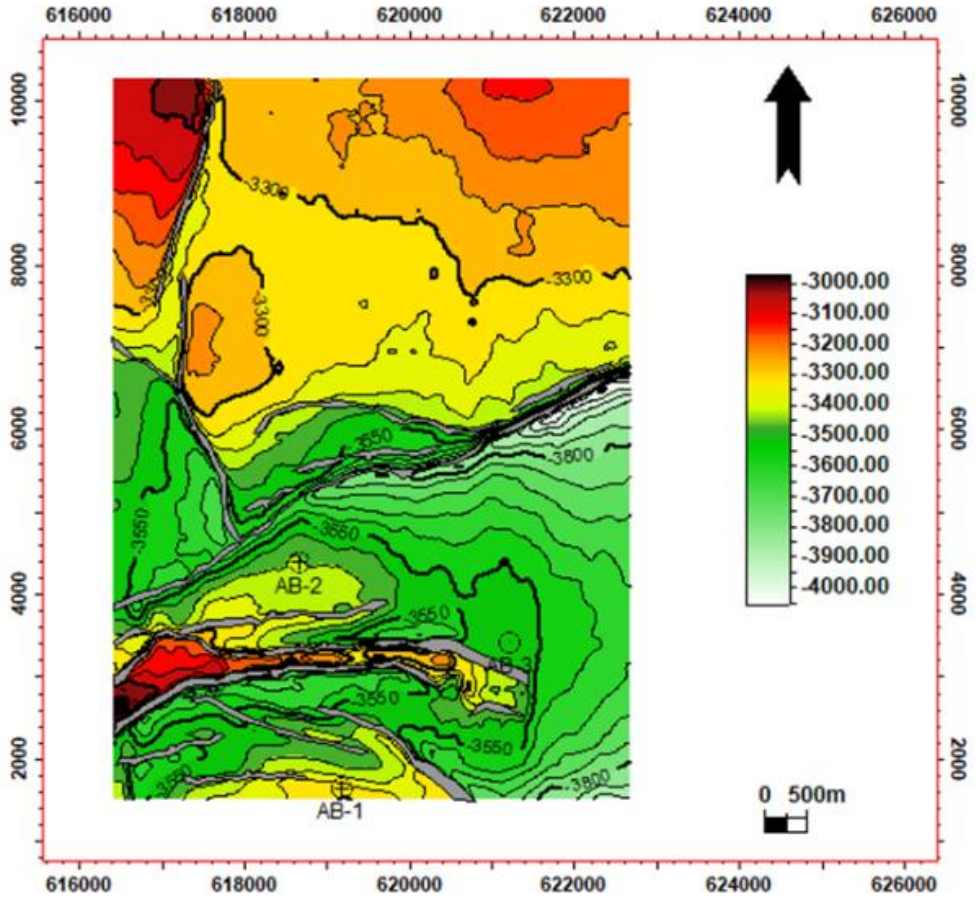


Figure 13: Reservoir B Depth Map

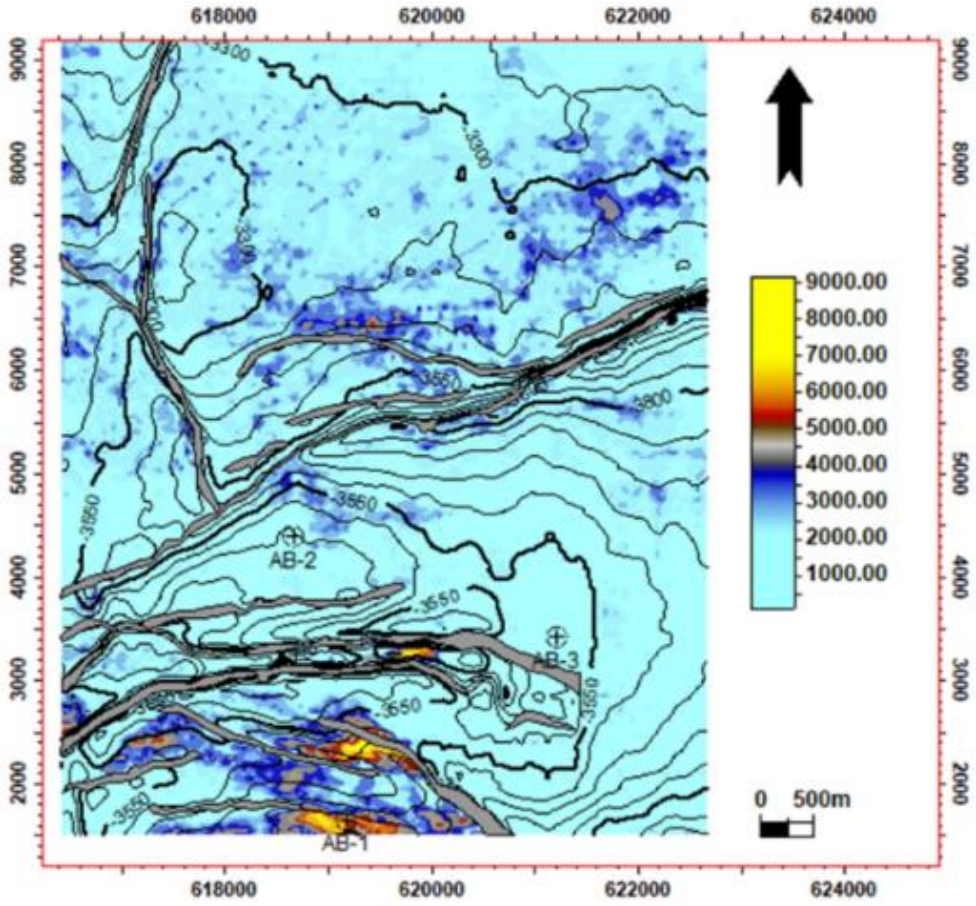


Figure 14: Reservoir B RMS Amplitude Map

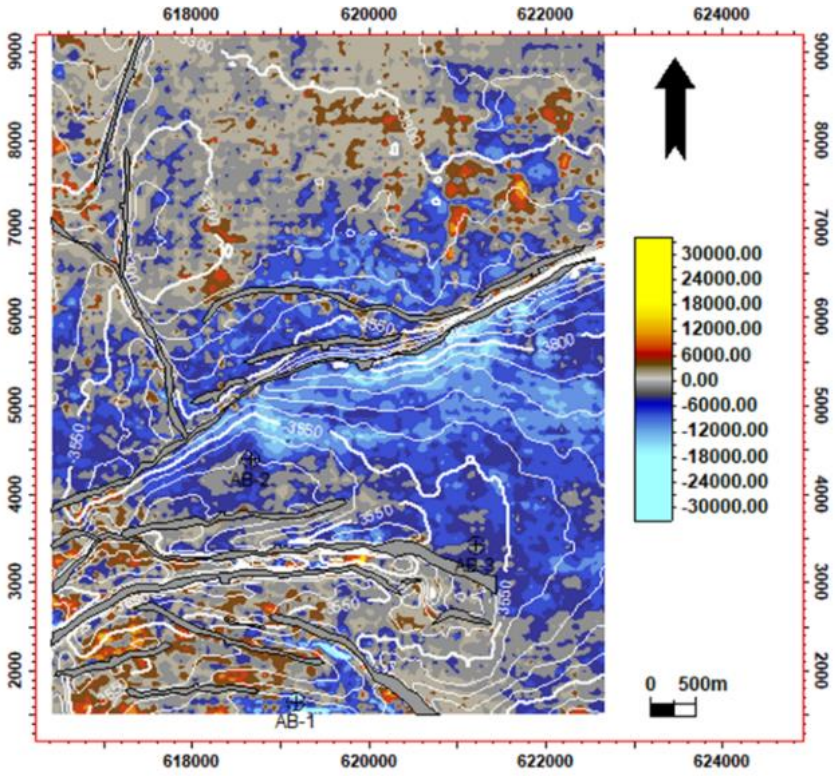


Figure 15: Reservoir B Minimum Amplitude Map

Reservoir C

Reservoir C time, depth, Root Mean Square (RMS) and minimum amplitude are presented below.

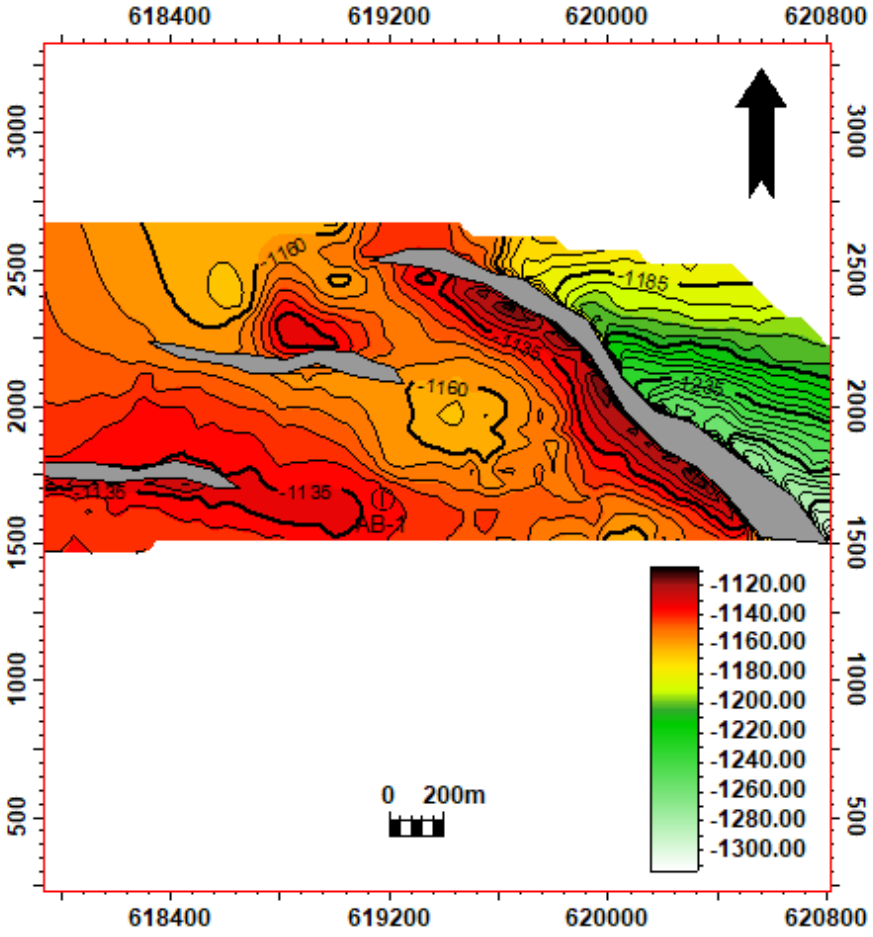


Figure 16: Reservoir C Time Map

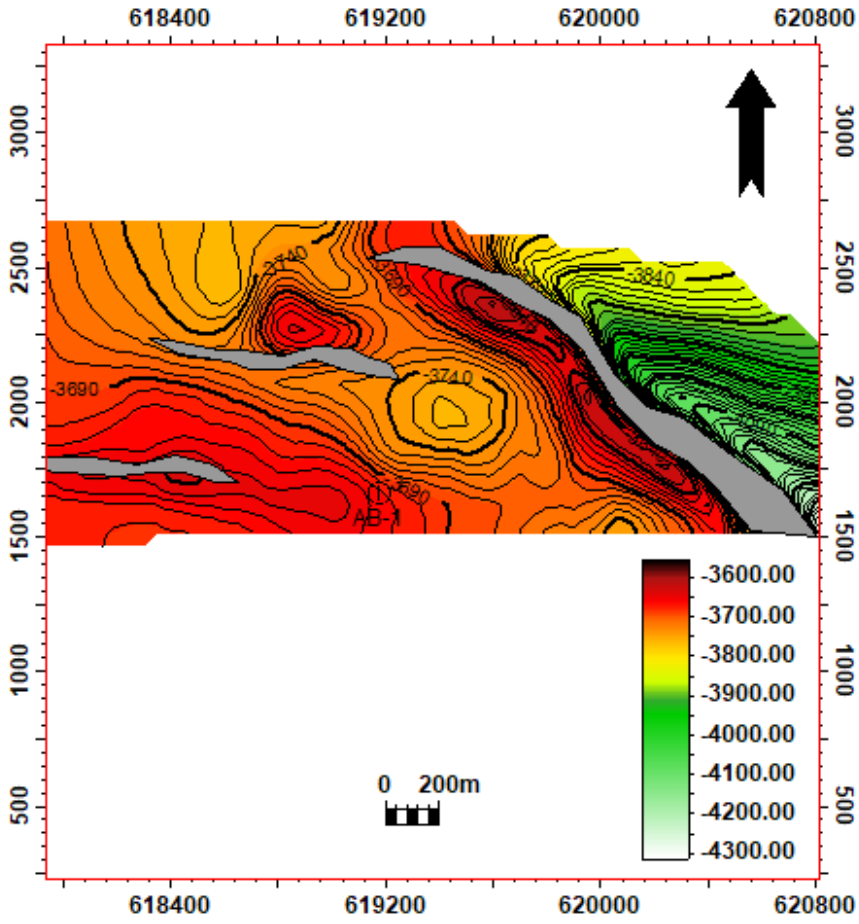


Figure 17: Reservoir C Depth Map

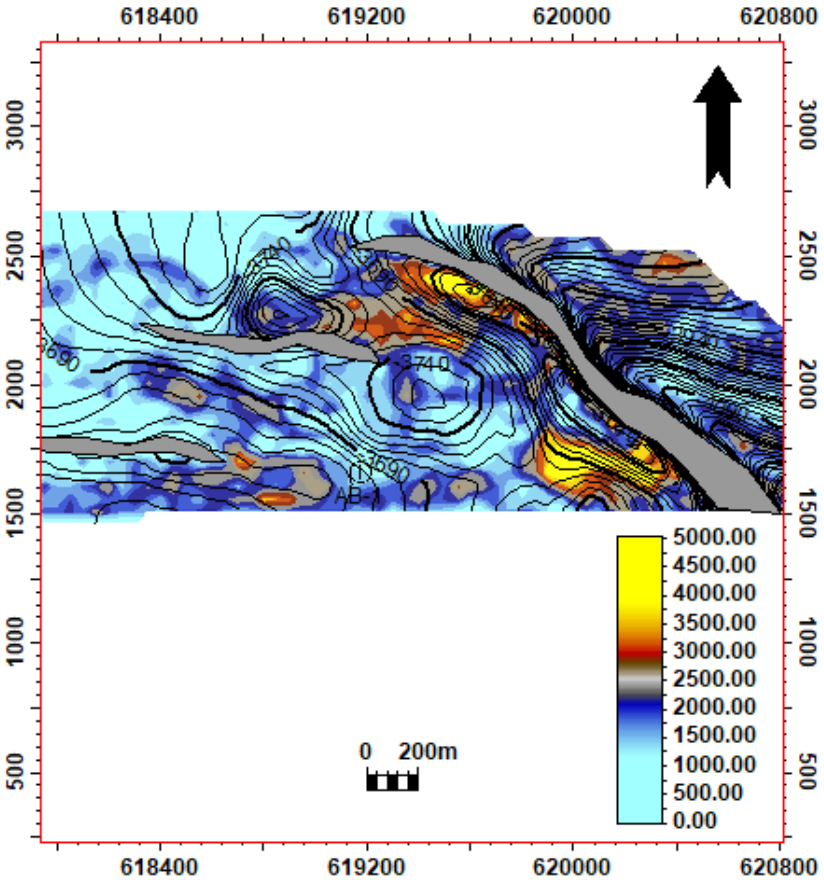


Figure 18: Reservoir C RMS Amplitude Map

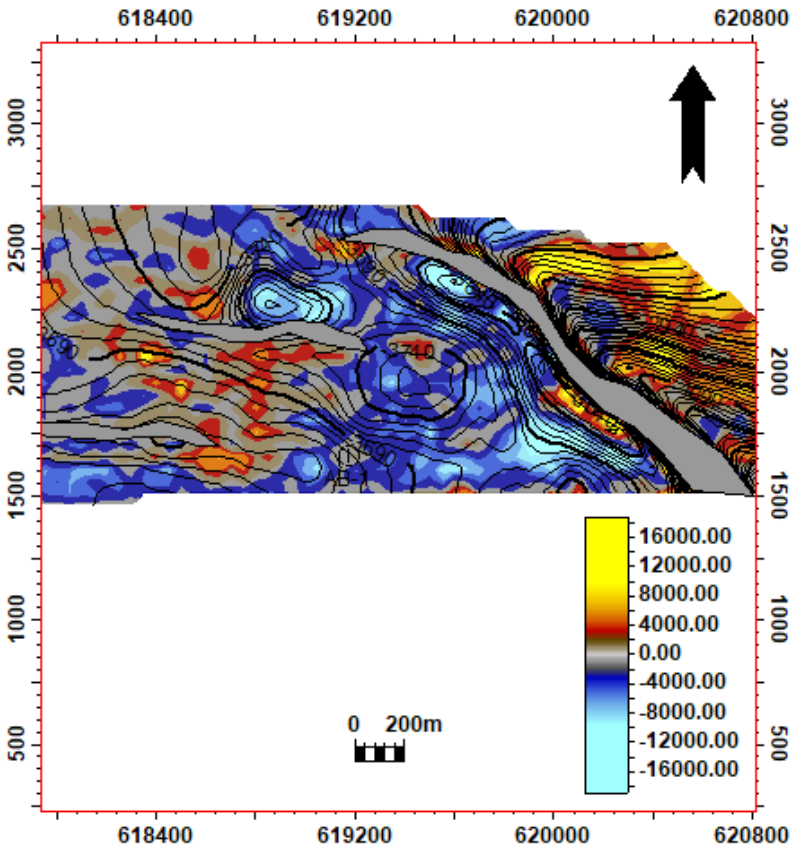


Figure 19: Reservoir C Minimum Amplitude Map

Reservoir G

Reservoir G time, depth, Root Mean Square (RMS) and minimum amplitude are presented below.

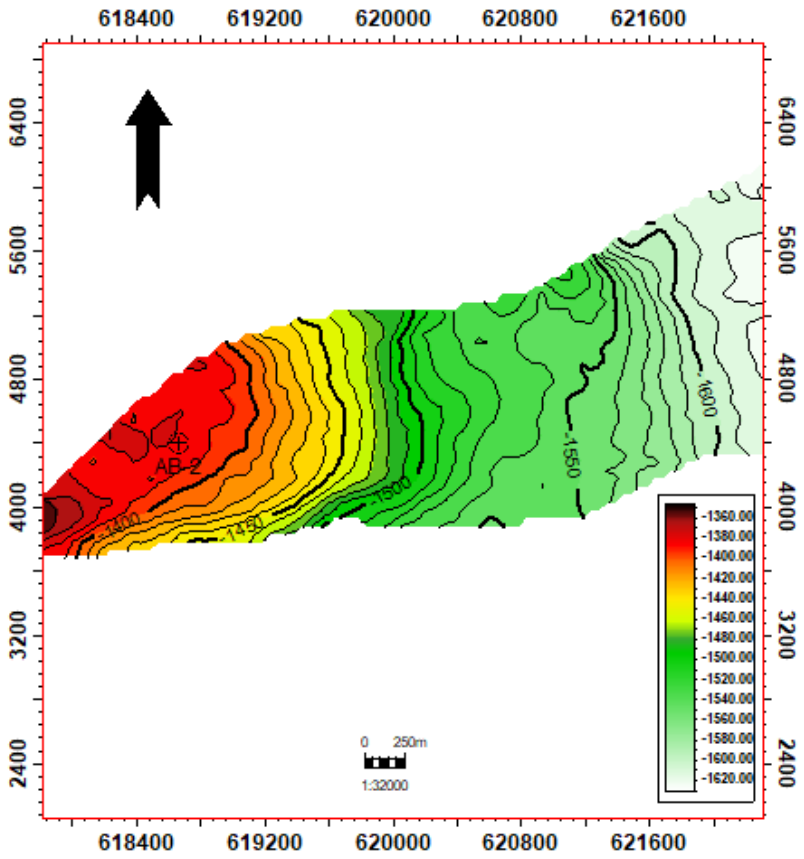


Figure 20: Reservoir G Time Map

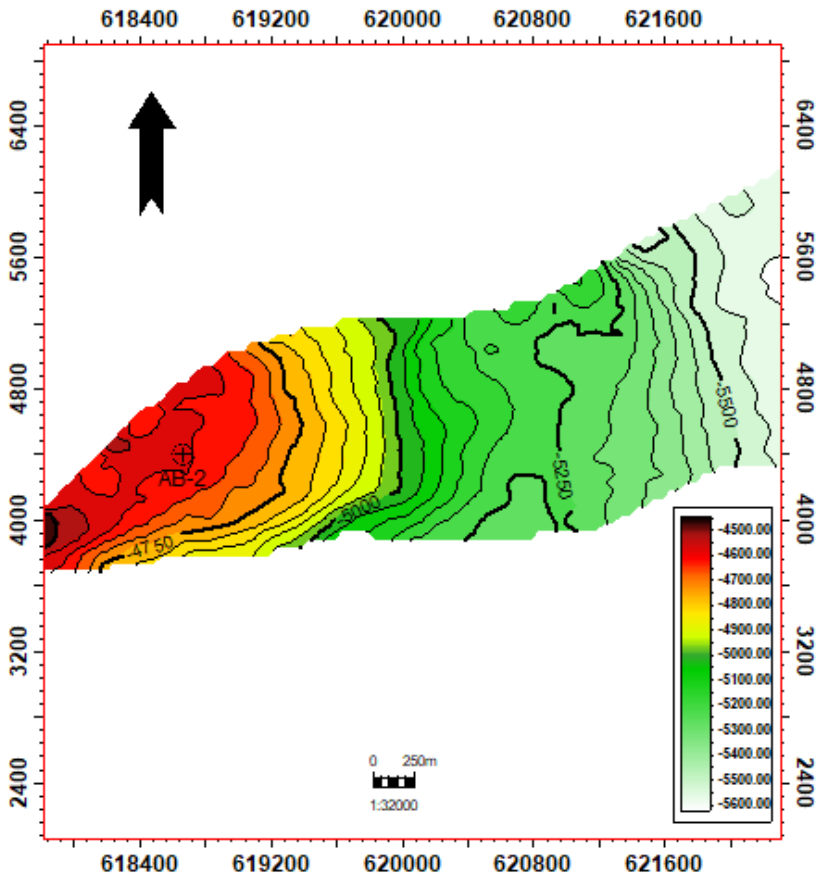


Figure 21: Reservoir G Depth Map

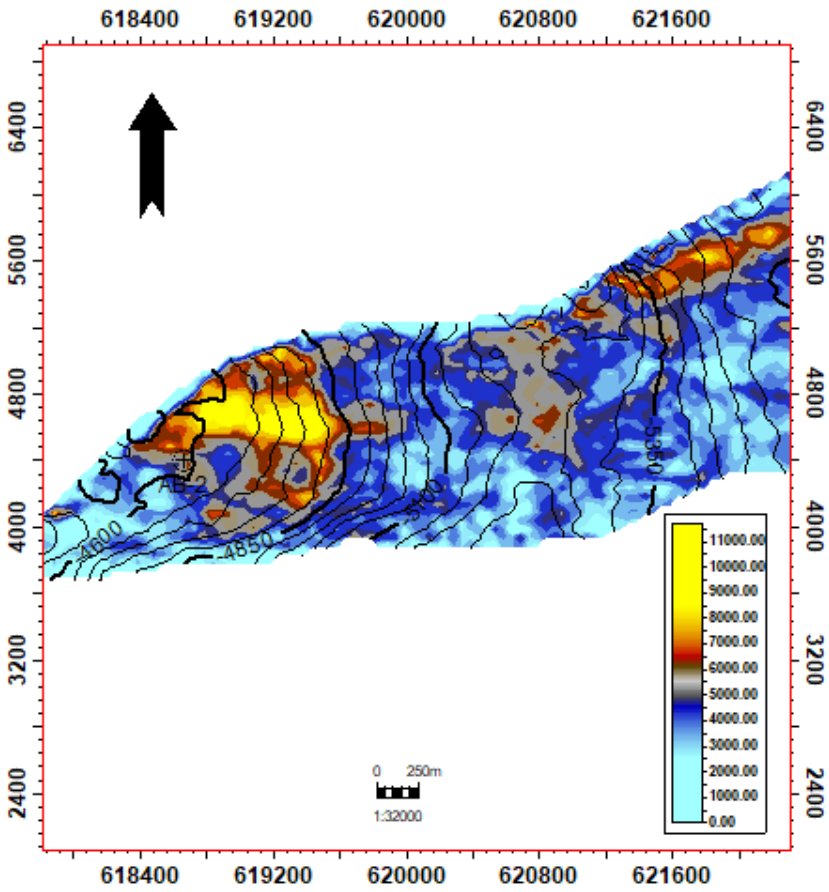


Figure 22: Reservoir C RMS Map

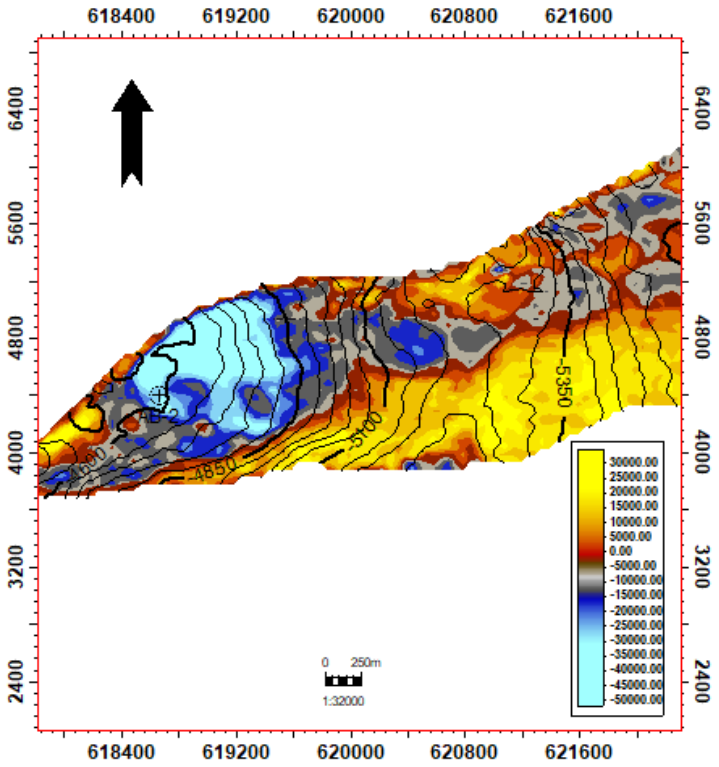


Figure 23: Reservoir C Minimum Amplitude Map

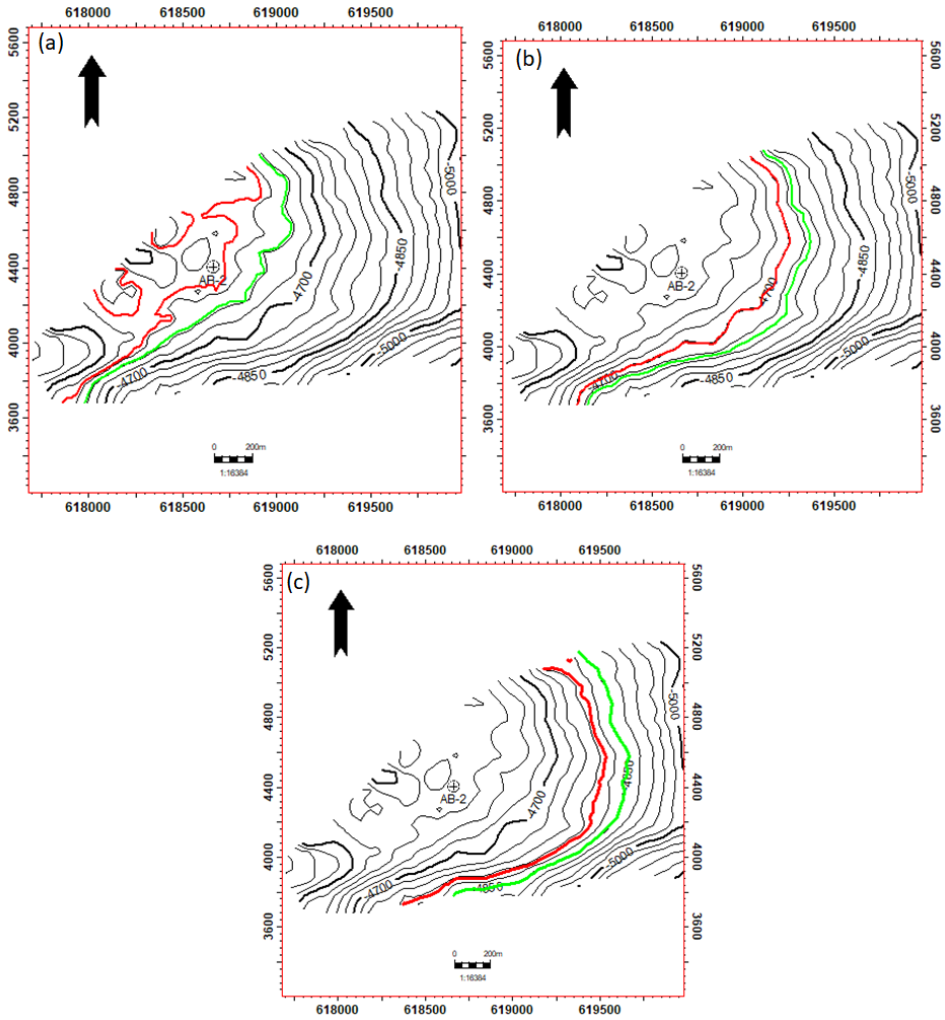


Figure 24: Realization of reservoir G depth structural map showing the (a) low case (b) base case (c) High case

Table 2: Contact information for Reservoir G and Predicted Hydrocarbon Height

RESERVOIR G CONTACT	GOC (ft)	OWC (ft)	PHH*(ft)
P10 (From neutron and density log)	-4600	-4634.68	74.68
P50 (mean of P10 andP90)	-4700	-4742.34	182.34
P90 (Seismic attribute)	-4800	-4850	290

*Predicted Hydrocarbon Height

Table 3: Petrophysical Evaluation

WELL	RESERVOIR	Gross thickness (ft)	Net Thickness (ft)	NTG	PHIT	PHIE	SW	VSH	PERM (mD)	Facies ID
ABU 1	Reservoir B	133	124.24	0.93	0.33	0.28	0.80	0.13	153.79	CS, USF, SH
	Reservoir C	222.50	192.75	0.86	0.31	0.27	0.42	0.11	470.24	CS, USF, SH
ABU 2	Reservoir G	45.50	11.50	0.25	0.29	0.24	0.36	0.15	579.11	LSF, SH

NTG = Net- To-Gross, PHIT =Total Porosity, PHIE = Effective Porosity, SW = Water Saturation, VSH = Volume of Shale, Perm = Permeability, CS = Channel Sand, USF = Upper Shoreface, LSF = Lower Shoreface, SH = Shale.

5.0 Discussion

5.1 ABU Structures

To assist the fault mapping process within the subsurface interval of ABU field, variance attribute was employed to better enhance and visualize the faults (Figure 10). Twelve of the fifteen faults that were mapped were synthetic, and the other three were antithetic. One of the major antithetic faults formed a graben in ABU-2 structure (Figure 11). Listric faults are the primary structural trap types in the Niger Delta, which are typical of the region's growth structures (e.g., Doust and Omatsola, 1990, Figure 2). Three faults are the major growth faults within the field which trends in NE- SW direction. These three major faults combine to form the three fault blocks in the field labelled A, B, C. The first fault block i.e. fault block A is at the hanging wall of fault block B and has been penetrated by ABU-2 well. There are two major structures present in the field i.e. ABU-1 and ABU-2 structures located in fault block A and C. These structures can be found in the study area's northern and southernmost sections.

Acoustic impedance seismic section along ABU-1 and ABU-2 in Figure 11 showing reservoir continuity depicts that reservoirs B and G are characterized by bright reflections. In summary, the bright reflections are associated with amplitude restriction within structural closures. Direct hydrocarbon indicator (DHI) support for hydrocarbon presence in the Niger Delta has been recognized for several decades and have been very effective across different geologic systems in the Niger Delta (Wojcik *et al.*, 2016).

5.2 Sequence Stratigraphy/ Facies Identification

The sequence-stratigraphic framework of wave-dominated deltaic reservoirs defines how their large-scale sedimentologic heterogeneity is organized (e.g., Hampson and Howell, 2017). Due to the presence of many laterally extensive and thin parasequence flow units, many wave-dominated deltaic reservoirs are susceptible to compartmentalization by sealing faults (e.g., Ainsworth, 2006, Reynolds, 2017), they are typical of growth fault-dominated deltaic plays dominated by Tertiary waves (e.g., Edwards, 1981; Rijks, 1981; Sydow *et al*., 2003).

In this study, two depositional cycles of the third order were found (Sequence 1 and Sequence 2) and the related system tracts from G-sand to B-

sand in the ABU field. The reservoir thickness at Reservoir G is seen to decline from the bottom up as upper shoreface and lower shoreface sands eventually cover the proximal channel sands. Based on this observation, the setting therefore depicts a transgressive marine environment. The usage of sequence stratigraphic analysis for prediction of depositional features is intended to reduce the uncertainty associated with prospects identification (Ogbe *et al*., 2020).

Three types of facies were found in reservoirs B and C, which contain channel sands, upper shoreface, and shales, and reservoir G, which includes lower shoreface, upper shoreface, and shales, as illustrated in figure 8. Channel and fan deposits can form good reservoirs because of their coarse sediment size and lateral continuity (Don *et al*., 2020).

5.3 Reservoir mapping and Attribute Analysis

Three (3) reservoirs (B, C and G) within a time window of about 950 ms – 1800 ms were mapped and were continuous across the seismics. Time and Depth Map were generated for the respective reservoirs using the aforementioned methodology (Figures 12, 13, 16, 17, 20 and 21). Out of the three reservoirs, only reservoir G was developed into a prospect because of its well-closed anticlinal structure compared to reservoir B and C. From the hydrocarbon typing logs (Density and Neutron porosity), reservoirs B, C and G most likely were gas, gas/oil and gas/oil respectively. However, the prominent reservoir G had most likely Gas-Oil Contact at -4700 ft and Oil Water Contact at -4742.34 ft with a base case predicted hydrocarbon height of 182.34 ft (Table 2). The Gas-Oil and Oil-Water contacts for the low, base and high cases were derived from Density-Neutron log; the mean of low and high cases; and Seismic minimum amplitude spill point respectively (Figure 24). This and other reservoirs were mapped in order to study the amplitude responses within associated fault blocks.

Horizon- based amplitude extraction was carried out for all the horizons mapped. The windows used for this extraction is restricted to the time window that corresponds to the reservoir gross thickness. Using the time window, the RMS amplitude extraction was carried out for all the reservoirs. In addition, Minimum amplitude was also generated based on the polarity type (Figures 14, 15, 18, 19, 22, 23 and 24).

The depth structure maps were overlain on the various attributes extracted in order to investigate if amplitude conform to structure. Amplitude conforms most likely to structure at Reservoir G – ABU-2 structure, fairly at Reservoir B – ABU-1 structure and poorly/patchy at Reservoir C – ABU-1 structure.

5.4 Petrophysical Evaluation

Table 3 displays the pay summary for the reservoirs, with a focus on Net-to-Gross, Total Porosity, Effective Porosity, Water Saturation, and Permeability in the ABU Field.

Total porosity values range from 29% to 33%, while the Net to Gross ratio (NTG) is between 0.25 and 0.93, the effective porosity ranges between 24% to 28%, Volume of Shale values are from 0.11 to 0.15, the range of Water Saturation is from 0.36-0.8 and Permeability ranges from 153.79mD to 579.11mD. The reservoirs have excellent quantitative results (Etu-Efeotor, 1997), with values ranging from 15% to 40% in the reservoir rocks, comparable to those reported for the Niger Delta. It was found that the sand intervals' reservoir properties decreased with depth. The growth faults regulate the reservoirs' thickness, which fluctuates laterally.

Comparatively, Reservoir B is most likely to be the best based on other properties, but the high-water saturation suggests a lower hydrocarbon saturation. Based on hydrocarbon saturation, Reservoir G is exceptional but have a very poor Net - to - Gross. This comprehensive data integration is crucial for robustly understanding reservoir properties, facies distribution and

heterogeneity in complex geological settings like the Niger Delta (Oluwadare *et al*., 2024).

6.0 Conclusion

This study centres on the reservoir characterization of the ABU field, focusing on Reservoirs B, C, and G. Reservoir G stands out as the most promising target for hydrocarbon production due to its well-defined anticlinal structure and strong petrophysical properties, despite having a lower Net-to-Gross ratio. Reservoir B also shows significant potential, especially because of its favourable petrophysical qualities, though its high-water saturation limits its hydrocarbon potential. Reservoir C, while continuous, doesn't offer the same advantages as the other two. By combining seismic and petrophysical data, we found that Reservoir G aligns best with the structural features, making it the top prospect for further development. In comparison, Reservoirs B and C show weaker conformance with the structure. Overall, even though Reservoir G has some sand distribution limitations, it remains the most favourable reservoir for exploration. while the ABU field's reservoirs are complex due to faulting and compartmentalization, Reservoir G provides the best opportunity for hydrocarbon extraction. This study offers significant information about the field's reservoir characteristics, which will be crucial for guiding future exploration and development.

Acknowledgements

The dataset utilized in this study was provided by EXXONMOBIL Nigeria plc, for which the first author is quite appreciative.

References

Ainsworth, R. B., (2006). Sequence stratigraphic-based analysis of reservoir connectivity: Influence of sealing faults – A case study from a marginal marine depositional setting, *in* Hampson, G.J., and Howell, J. A., (2017). Sedimentologic and sequence-stratigraphic characteristics of wave-dominated deltas: AAPG Bulletin, v.101, no. 4, p. 441 – 451.

Aminu, M. B. and Olorunniwo, M.A., (2011). Reservoir characterization and paleo-stratigraphic imaging over Okari Field, Niger Delta, using neural networks: The Leading Edge, 30, no. 6, 650-655.

Bedle, H.; Chopra, S. and Davis, T.; (2024). Introduction to this special section: Reservoir Characterization. The Leading Edge, Vol. 43, No. 12: 798-799.

Beka, F.T. and Oti, M.N., (1995). The distal offshore Niger Delta: Frontier prospects of a mature petroleum province, in: M.N. Oti and G. Postma, eds, Geology of Deltas: A.A. Balkema, 237-241.

Boggs, S., (2006). Principles of Sedimentology and Stratigraphy. Pearson Prentice Hall, Pearson Education Inc, U.S.A., 662P.

Burke, K., Dessauvagie, T.F.J., and Whiteman, A.J., (1971). Opening of the Gulf of Guinea and geological history of the Benue Depression and Niger Delta: Nature, 233, 140 – 142, doi: 10.1038/233140a0.

Bjorlykke, K. (2015). Petroleum Geoscience. Springer-Verlag, Berlin Heidelberg. 662P.

Cant, D. J., (1992). Subsurface facies analysis, *in* Walker, R.G., and James, N.P., eds., Facies models: Response to sea level change: pp. 27 – 45. Geological Association of Canada.

Cartwright, J.A., Bouroullec, R., James, D. and Johnson, C.S., (1998). Polycyclic motion history of some Gulf Coast growth faults from high resolution

displacement analysis: Geology, v. 26, p. 1425 – 1432.

Chopra, S. and Michelena, R.J., (2011). Introduction to this special section: Reservoir Characterization. The Leading Edge, 30(1): 35-37.

Cross, T.A. and Lessenger, M.A., (1998). Sediment volume partitioning: rationale for stratigraphic model evaluation and high-resolution stratigraphic correlation, *in* Gradstein, F. M., Sandvik, K.O., and Milton, N.J., eds., Sequence stratigraphy – Concepts and applications: Norwegian Petroleum Society Special Publication 8, p.171-195.

Damuth, J.E., (1994). Neogene gravity tectonics and depositional processes on the deep Niger Delta continental margin: *in* Pochat, S., Castelltort, S., Van Den Driessche, J., Besnard, K., and Gumiaux, C., (2004). A simple method of determining sand/shale ratios from seismic analysis of growth faults: An example from upper Oligocene to lower Miocene Niger Delta deposits. AAPG BULLETIN, v. 88, no. 10, pp. 1357 – 1367.

Doust, H. and Omatsola, E., (1990). Niger Delta in J. D. Edwards and P.A. Santogrossi, eds., Divergent/Passive margins basin: AAPG Memoir, 48, 201 – 238.

Edwards, M.B., (1981). Upper Wilcox Rosita delta system of South Texas: Growth-faulted shelf-edge deltas, *in Hampson*, G.J., and Howell, J. A., (2017). Sedimentologic and sequence-stratigraphic characteristics of wave-dominated deltas: AAPG Bulletin, v.101, no. 4, p. 441 – 451.

Edwards, M.B. (1995). Differential subsidence and preservation potential of a shallow water Tertiary sequences, northern Gulf Coast basin, U.S.A.: Special Publication of International Association of Sedimentology, v. 22, p. 265-281.

Etu-Efeotor, J.O., (1997). Fundamentals of petroleum geology. Paragraphics, Port-Harcourt, Nigeria, 146P.

Hampson, G.J. and Howell, J. A., (2017). Sedimentologic and sequence-stratigraphic characteristics of wave-dominated deltas: AAPG Bulletin, v.101, no. 4, p. 441 – 451.

Jessica D., Shaw, J.H., Plesch, A. Daniel, D. B. & Lufadeju, G. (2020). Characterizing the growth of structures in three dimensions using patterns of deep-water fan and channel systems. AAPG BULLETIN, v. 104, No. 1, pp. 177 – 203.

Lawrence, S. R., Munday, S. and Bray, R., (2002). Regional geology and geophysics of the eastern Gulf of Guinea (Niger Delta to Rio Muni): The Leading Edge, V. 21, no. 11, pp. 1112- 1117.

Lowrie, A., (1986). Model for fine-scaled movements associated with climate and sea-level changes along Louisiana shelf-break growth faults: Transactions of the Gulf Coast Association of Geological Societies, v. 36, p. 497 – 509.

Mitchell, N.C., (1996). Creep in pelagic sediments and potential for morphologic dating of marine fault scarps: Geophysical Research Letters, v. 23, p. 483 – 486.

North, F.K. (1985). Petroleum geology, Unwin Hyman Inc. 631P.

Oluwadare, O.A., Folorunso, A.F. Ashiru, O.R. and OtoAbasi-Akpan, S.I. (2024).

High resolution 3-D seismic and sequence stratigraphy for reservoir prediction in 'Stephi Field', offshore Niger Delta, Nigeria. Scientific reports, 14: 22390.

Ovie B. O, Iheanacho P. O., Jerry, O., Tuviere O. and Sunday E. O, (2020). Interaction between sea-level changes and depositional tectonics: Implications for hydrocarbon prospectivity in the western coastal swamp depobelt, Niger Delta Basin, Nigeria. AAPG BULLETIN, v. 104, No. 3, pp. 477 – 505.

Reading, H.G., (1986). Sedimentary Environment & Facies. Blackwell Scientific Publications, 2nd Edition, 615P.

Reynolds, A.D., (2017). Paralic reservoirs, *in* Hampson, G.J., and Howell, J. A., (2017). Sedimentologic and sequence-stratigraphic characteristics of wave-dominated deltas: AAPG Bulletin, v.101, no. 4, p. 441 – 451.

Rijks, E. J. K., (1981). Baram Delta geology and hydrocarbon occurrence, *in* Hampson, G.J., and Howell, J. A., (2017). Sedimentologic and sequence-stratigraphic characteristics of wave-dominated deltas: AAPG Bulletin, v.101, no. 4, p. 441 – 451.

Soreghan, M.J., Scholz, C.A. and Wells, J.T., (1999). Coarse-grained, deep-water sedimentation along a border fault margin of Lake Malawi, Africa: Seismic stratigraphic analysis: Journal of Sedimentary Research, v. 69, p. 832 – 846.

Stacher, P., (1995). Present understanding of the Niger Delta hydrocarbon habitat, in, Oti, M.N., and Postma, G. eds., Geology of Deltas: Rotterdam, A.A. Balkema, P. 257 – 267.

Sydow, J. C. J., Finnerman, J. and Bowman, A. P. R., (2003). Stacked shelf-edge reservoirs of the Columbus Basin, Trinidad, West Indies, *in* Hampson, G.J., and Howell, J. A., (2017). Sedimentologic and sequence-stratigraphic characteristics of wave-dominated deltas: AAPG Bulletin, v.101, no. 4, p. 441 – 451.

Udoh, A.C., Bassey, C.E., Ekot, A. E. and Udoh, M.U. (2020). Sequence Stratigraphic Study of 'X' Field in Eastern Niger Delta, Nigeria. Journal of Geology and Mining Research, Vol. 12(2), pp. 65 – 79.

Udoh, A. and Udoh, M. (2020). Sequence Stratigraphy of Some Parts of Niger Delta, Nigeria. LAP, Lambert Academic Publishing, Schaltungs-dienst Lange o. H.G., Berlin, pp. 1 – 62.

Udoh, M. U. Umaru, A. F., Chukuyen, O. P., Jigo, H. B., Ogamba, U. &Udoh, A. C. (2017). Seismic Facies Interpretation of 'X' and 'Y' Fields, Central Depobelt, Niger Delta, Nigeria. International Basic and Applied Research Journal, Vol. 3, No. 1, pp. 1-20.

Udoh, M. U., Ogba, E. A., Udoh, A. C., Tsaka, S. S. and Dongo, M. E. (2017). Sequence Stratigraphic Study and Reservoir Prediction of Ekazy Field, Greater Ughelli Depobelt, Niger Delta, Nigeria. International Basic and Applied Research Journal, Vol.3, No. 5, pp. 1-15.

Webb, H.F. and Jordan, T.H. (2001). Pelagic sedimentation on rough seafloor topography: 1. Forward model: Journal of Geophysical Research, v. 106, no. B12, p. 30,433- 30,449.

Wojcik, K.M., Espejo, I.S., Kalejaiye, A.M. and Umahi, O.K., (2016). Bright spots, dim spots: Geologic controls of direct hydrocarbon Indicator type, magnitude and detectability, Niger Delta Basin. Interpretation, Vol. 4, No. 3, p. SN45-SN69.